Suspicious Lesion Detection in Mammograms using Undecimated Wavelet Transform and Adaptive Thresholding

Abhijit Nayak, Dipak Kumar Ghosh, Samit Ari
Department of Electronics & Communication Engineering
National Institute of Technology, Rourkela, 769 008, India
E-mail: abhijitnayak25@gmail.com, dipakkumar05.ghosh@gmail.com, samit.ari@gmail.com
Telephone: +91-661-2464/4464

***Abstract*—Mammographic screening is the most effective procedure for the early detection of breast cancers. However, typical diagnostic signs such as masses are difficult to detect as mammograms are low-contrast noisy images. This paper proposes a systematic method for the detection of suspicious lesions in digital mammograms based on undecimated wavelet transform and adaptive thresholding techniques. Undecimated wavelet transform is used here to generate a multiresolution representation of the original mammogram. Adaptive global and local thresholding techniques are then applied to segment possible malignancies. The segmented regions are enhanced by using morphological filtering and seeded region growing. The proposed method is evaluated on 120 images of the Mammographic Image Analysis Society (MIAS) Mini Mammographic database, that include 89 images having in total 92 lesions. The experimental results show that the proposed method successfully detects 87 of the 92 lesions, performing with a sensitivity of 94.56% at 0.8 false positives per image (FPI), which is better than earlier reported techniques. This shows the effectiveness of the proposed system in detecting breast cancer in early stages.**

***Keywords*— Adaptive thresholding, computer-aided diagnosis (CAD), lesion detection, mammography, undecimated wavelet transform.**

I. Introduction

Breast cancer is the leading cause of cancer deaths among women worldwide. In 2008, mortality in case of breast cancer accounted for 13.7% of all cancer deaths in women [1]. In 2008, incidence rates for women of all age groups in India was reported to be 22.9%. The incidence-to-mortality ratio was about 2:1, which is significantly higher than that of the United States for the same period. Research has shown that regular screening can significantly lower mortality rates. Mammography is considered to be the most reliable detection method for screening breast cancers. Cancers vary in appearance and size in early stages which makes Computer Aided Diagnosis (CAD) an important tool in assisting doctors in the early detection of cancers [3]. CAD provides another dimension to doctors' point of view, thereby minimising the chances of missing out a positive cancerous region. Based on mammograms, breast cancers are characterised and classified by the two primary signatures (a) microcalcifications, and (b) space-occupying lesions. Microcalcifications are tiny deposits of calcium that occur as small bright spots in a mammogram. Space occupying lesions are described by their shape and margin properties. These are often indistinguishable from the surrounding glandular tissue because of similar attenuation properties. Based on this classification, CAD systems generally consist of two subsystems, *i.e.*, for the detection of microcalcifications and masses respectively. In this paper, we focus on the detection of masses.

Space occupying lesions are classified into masses, architectural distortion (ARCH) and asymmetry (ASYM). Maees are further subdivided into spiculated masses (SPIC), circumscribed masses (CIRC), and other masses (MISC) based on shape and margin features. Lesions with smooth margins are typically benign, whereas malignant masses often show spiculated boundaries developed over time. Masses normally range from 3mm to 50mm [4]. Sometimes, masses appear as blurred objects. They have high intensity values locally but on the lower side of intensity values on a global scale. This explains why only global thresholding based on the average intensity of the image is insufficient to produce the required results. Thereby thresholding on a local scale is indispensable in such cases.

A large number of image processing algorithms [7]–[10] have been proposed in the literature for suspicious lesion detection in mammograms. These basically use three properties of masses–shape, texture and gray level or intensity. Detection of lesions is the first step in mammographic analysis. The following step is usually the determination of the subtype of masses using classification techniques. Fathima *et al.* [5] have proposed a method for classification of tumors by training an SVM classifier with a number of features extracted for the Region of Interest (ROI). In this work, we focus on the detection process. Image enhancement techniques have been shown to be highly effective in increasing the efficiency of mass segmentation methods [6]. Brake *et al.* [7] identified stellate distortions by using orientation map of line-like structures and subsequently marking the location of suspicious malignant regions. Zhang and Desai [8] used multiresolution analysis along with a Bayes classifier to identify possible tumours. Kom *et al.* [9] proposed a contrast enhancement algorithm based on

linear transformation filters and a local thresholding approach based on a small and a large window around the pixel to detect possible masses. Hu *et al.* [10] used a multiscale image analysis followed by adaptive global and local thresholding based on empirically chosen parameters to detect suspicious malignant masses. Mencattini *et al.* [11] proposed an algorithm to detect masses in low contrast images by using orientation of gradient vectors in the image rather than their amplitude. Many of the methods described here have limited scope due to the approach used or because of the specificity of the algorithm, *e.g.*, algorithms designed specifically for detection of spiculated masses.

In this paper a novel detection method based on multiresolution analysis using undecimated 2D wavelet transform (UWT) is proposed. The method improves detection results by using the translation invariance property of UWT. Processing of an image by UWT involves much less noise than classical DWT. One of the crucial advantages of using UWT is that we get a perfect reconstruction with minimal loss of information which could be used for further analysis. Also, for a detection process, the applied thresholding criterion cannot be the same for all the images. For any given image, parameters should vary according to the values of some predetermined features. Since these values would be specific to that image, the parameters involved in the algorithm would be different for each image. To achieve this objective, adaptive global and local thresholding are applied to select the suspected regions. Then the segmented regions are enhanced using region growing. The method has been tested on images from the Mini MIAS Database [16] and the experimental results are better as compared to earlier reported techniques [10].

The rest of the paper is organized as follows. Section II explains the whole proposed system in detail. The results obtained by the proposed method are presented in Section III. Finally, Section IV concludes the work.

II. Proposed Methodology

Fig. 1 represents the block diagram of the proposed methodology. The details of the methodology are given below.

A. Artefacts and Pectoral muscle removal

Mammograms often contain labels and artefacts which occur as high intensity marks on a dark background. These along with noise can affect the results of the detection algorithm. These are of no particular significance for mass detection. Hence these must be removed using suitable methods. Generally they are disconnected from the breast area. This feature is exploited in the label removal process. We use the largest area criterion as described in [14] after a binary thresholding to separate out the label marks from the large breast region. Pectoral muscle is a dense muscle close to the chest that occurs on the opposite side of the nipple in a mammogram. It has significantly high intensity levels which might affect the parameters related to the breast region. Due to high gray levels, it occurs as remnant blocks or false positives in the result. The pectoral muscle does not belong to the actual breast region

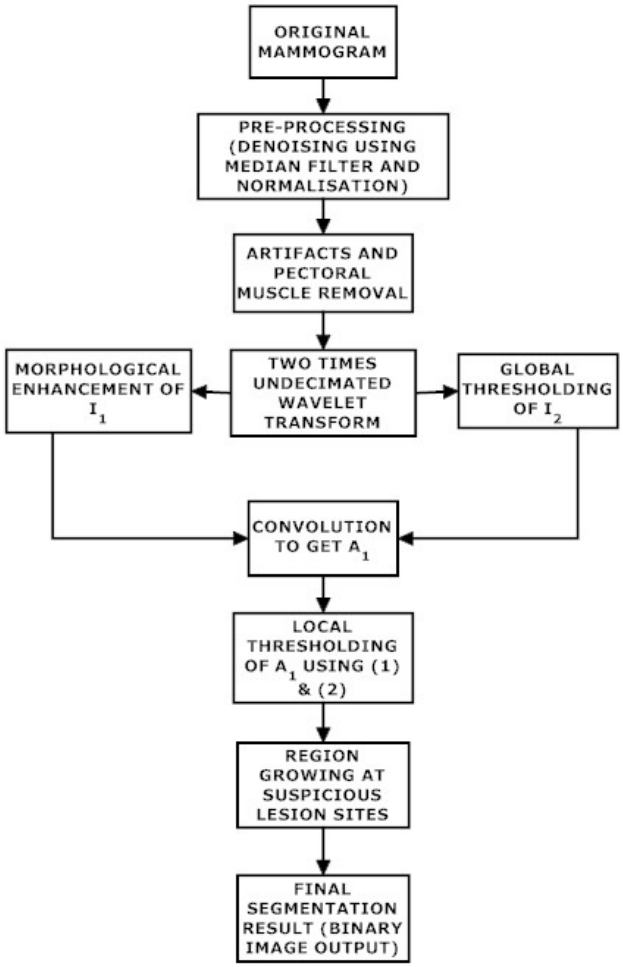

Fig. 1. The flow-chart depicting the steps involved in the proposed method

and probability of a mass lying inside or adequately close to it is negligible. Hence, removing it improves the segmentation results. We determine the orientation of the breast and then use Single-Seeded Region Growing for pectoral muscle removal [14]. The steps involved in the removal of artefacts and pectoral muscle are shown in Fig. 2.

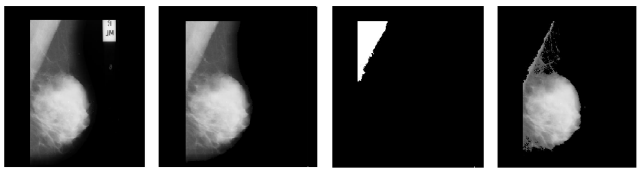

Fig. 2. Breast region segmentation for mdb002. (a) Original mammogram (b) Removal of artefacts (c)Region to be segmented out as pectoral muscle (d) Output after the removal of pectoral muscle

B. Global thresholding and morphological enhancement

Prior to global thresholding and morphological filtering, we apply wavelet processing to the image and select the

images reconstructed from the $1st$ and $2nd$ level approximation coefficients for further processing. Multiresolution analysis extracts the image details at different scales. Wavelet processing of images (2-D) and PDF curves (1-D) removes singularities and noise and smoothens and enhances the fearures for further processing. The biorthogonal wavelet transform performs poorly in case of analysis procedures like filtering and detection. This is mainly due to the loss of translation-invariance. As a result, the output obtained after reconstruction (from the processed transform coefficients) contains a large number of artefacts and noise elements. This alters the original information contained in the image and also causes faulty detections in the form of false positives. This can severely affect the efficiency of the detection method [12]. In this work, we propose a lesion detection method based on the Undecimated Wavelet Transform (UWT). This representation uses the same filter banks as a biorthogonal wavelet transform, except that there is no sub-sampling of coefficients. As no coefficient is omitted, there is no need to perform interpolation by zeroes while reconstructing the image for further processing. This inherently redundant process is completely translation-invariant. This property is very crucial for methods like segmentation processes where minute details can affect the results significantly. It has also been exploited for signal denoising processes. [13]We use Daubechies wavelet (Db 10), used in [10] for generating the transform coefficients. For the processing of PDF curves to generate the global threshold, we apply one-dimensional UWT using Daubechies 6-point (Db 6) wavelet. These are reported to be fairly good for signal denoising processes [15].

The adaptive global thresholding used in this method is based on the probability density function of I_2, the image reconstructed from the 2^{nd} level UWT coefficients of the original image. They are 256 intensity levels in total, ranging from 0 to 255 (8-bit accuracy). The basic idea is to identify a valley region between two portions having significant share among all the intensity levels in the PDF. The minima at this region is shown to be fairly close to the Bayes threshold [8]. In case the PDF curve is not evidently bimodal in nature, and there is greater overlap between the peaks, the minima of the derivative of the PDF curve is used to calculate the global threshold for the image [10]. After that the pixels are classified according to the criteria given in (4). This gives a binary output, which is later convolved with the output obtained by morphologically enhancing I_1 to get A_1. The morphological enhancement methodology is taken from [4]. The output obtained after the convolution process is shown in Fig. 3 (c). Global thresholding essentially serves two purposes in this method. First, since the adaptive threshold uses intensity level features of the histogram, it ensures that masses, which often have gray levels on the higher side of histogram, are present in the segmented binary image. Secondly, it reduces the number of computations by creating a subset of pixels from all the pixels in the image, which is then further processed using local thresholding, thus making the process more time-efficient. Fig. 3 (b) shows the output after global thresholding for three mammograms with spiculated lesions.

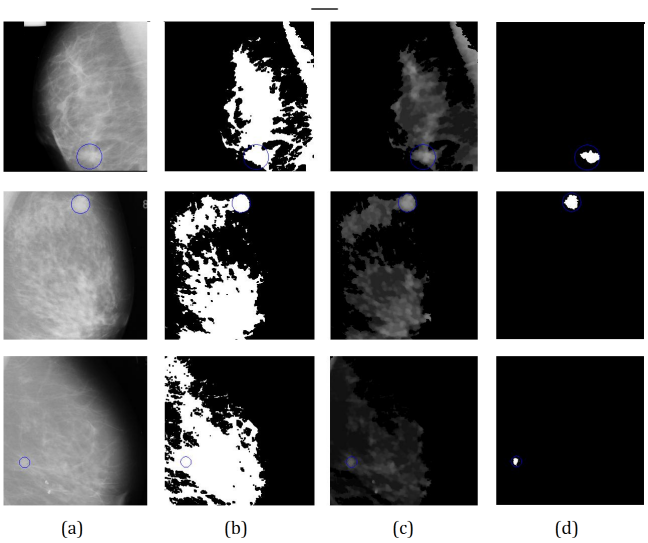

Fig. 3. Detection results for SPIC lesions. From top to bottom are the cases of mdb181, mdb202, and mdb204, respectively. (a) Original mammograms (b) After global thresholding. (c) Convoluted images. (d) Final output.

C. Local thresholding

As discussed before, masses are centres of locally higher gray levels. Therefore, processing of the image by focussing on small local regions, preferably variable in size, is very crucial. In this method, we use the windows-based adaptive local thresholding method as described in [10]. For each pixel of A_1, one small and one large window containing it are defined, and a distinct threshold value is calculated based on (1) and (2). A pixel is classified as a potential suspicious region if $SI(i,j) \geq TH(i,j)$ and $SI_{dif} > MvoisiP$, where $TH(i,j)$ is the threshold value for the pixel at (i,j), and $SI(i,j)$ is its intensity value. MvoisiP is the mean intensity of the small window, and SI_{dif} is defined as the difference in the maximum and minimum intensity values in the large window (II-C). The threshold value is calculated as follows.

$$TH(i,j) = \begin{cases} \alpha.MvoisiP, & if\ MvoisiP > SI(i,j) \\ MvoisiP & otherwise \end{cases} \quad (1)$$

else

$$TH(i,j) = MvoisiP + \gamma.SI_{dif} \quad (2)$$

with

$$SI_{dif} = SI_{max}(i,j) - SI_{min}(i,j)$$

where α and γ are the thresholding bias coefficients. In particular, α is used as a decision threshold to determine and evaluate the accuracy of the system by generating FROC curves.

D. Region Growing

As we increase the value of α, a reduction in the number of falsely detected regions is noticed. This improves the specificity. However, the areas of correctly detected regions also decrease simultaneously. Sometimes the overlapping criteria used to classify regions as true detections might not be satisfied, thereby affecting efficiency. To avoid this, we apply region-growing on the final image with an empirically determined threshold. This aims at readjusting the size of the detected regions. It adds new pixels to the region based on the similarity of their intensity levels. This also improves the shape pattern of detected lesions. They are less dependent on the shape of structural element used in morphological processing. After the local thresholding, the algorithm takes the segmented areas in the output as the initial seeds. To avoid the inclusion of high intensity non-lesion components like ducts or other trivial components, we perform morphological opening and closing operations on the final image. Fig. 3 (d) shows the final output after local thresholding and region growing.

III. Experimental results and discussions

The data set used in the experiment is taken from the Mammographic Image Analysis Society (MIAS) [16]. It consists of 322 images in total out of which 90 images have real space occupying lesions. All images are digitized at 200 micron pixel edge at a resolution of 1024 X 1024 pixels and eight-bit accuracy (gray level). The algorithm is implemented in a MATLAB environment on a computer with Intel Core i3 processor, 2.53 GHz CPU and 2 GB RAM. It is tested on 120 mammograms from the Mini MIAS database out of which 89 images contain space-occupying lesions. [1] Among these, 22 images contain CIRC lesions, 19 contain SPIC lesions and 14 contain MISC lesions. There are 19 and 15 images of ARCH and ASYM types respectively. We used the percentage area overlap criteria in [10] to evaluate the results against the ground truth.

Among these images, sensitivity level varies amongst various classes of lesions. The algorithm performs with a sensitivity of 100% in case of MISC and ASYM. This is because these are primarily classified by their distinct gray levels. Thus local thresholding proved to be highly efficient. In the case of CIRC lesions, a good sensitivity of 95.8% is achieved owing to their nearly oval shapes. These shapes are readily enhanced by the morphological filter. On the other hand, SPIC and ARCH lesions are generally characterised by their texture and boundary features. They vary a lot in size and pattern. Gray-level based criteria is not the best approach in this regard as many lesions have low to moderate intensity. This makes classification using intensity based thresholding relatively difficult. Also, a greater number of false positives is seen in these types.The system showed a sensitivity of 89.5% among both SPIC and ARCH type abnormalities. At a sensitivity of 91.3%, the FPI of the proposed method wa found to be 0.7, slightly better than [10]. The system reached a highest sensitivity of 94.56% at 0.81 FPI. The smallest lesion detected by the proposed method is a spiculated lesion in the image mdb206 having an approximate radius of 17 pixels, which is the smallest lesion size in the whole dataset. But smallest detectable size is not a measure of the efficiency of the system. This is because lesions with greater sizes also might not be detected on account of unusual shapes and surrounding tissues with similar gray levels.

These results are compared to those obtained by Hu *et al.* and summarised in Table I. We have compared the results of 54 images with abnormalities to the corresponding results provided by Hu *et al.* in [10], and also with a previous method by Cao *et al.* [17] in which the same database was used. Table II shows the comparison results. It gives the number of suspicious targets detected in the images, however details on whether it is a true detection or a false positive is part of the second part of the process and not shown here.

TABLE I
Results of the proposed method compared with those of Hu *et al.* [10]

Class of Abnormality	Sensitivity (%)	
	Hu *et al.* [10]	Proposed Method
CIRC	95.8	95.8
SPIC	78.9	89.5
ARCH	94.7	89.5
ASYM	93.3	100.0
MISC	93.3	100.0
TOTAL	91.3	94.56

FROC analysis is considered the most comprehensive method in evaluating the accuracy of a diagnostic test [18]. The sensitivity-specificity pair describes diagnostic accuracy more meaningfully than a single index of percentage correct, and has been used widely in the medical literature. FROC curves allow the possibility of more than 1 lesion per image. Data are collected in terms of a confidence rating provoded by the decision maker. The horizontal axis of a FROC curve, unlike general ROC curves, is not normalized to a maximum value of 1.0. This is in order to accomodate a large number of false-positive reports per image. The FROC analysis of the proposed method is shown in Fig. 4. Here, the vertical axis represents the true positive fraction (TPF). This gives a measure of the sensitivity of the algorithm (ratio of the number of lesions detected to the total number of lesions). The horizontal axis represents the average number of false positives per image. It is a measure of specificity. FROC curves are generated by using different values for α, the decision threshold here. Accordingly, the TPF and FPI vary.

The proposed method uses the shift-invariant undecimated wavelet transform to process the mammograms in two levels. UWT is responsible for suppressing noise elements and artefacts, which in turn increases the sensitivity of the algorithm by allowing minimal distortion in the original data. It also

[1] Due to non-availability of ground truth for the image mdb059, only 89 of the 90 images have been used in the experiment.

TABLE II
NUMBER OF SUSPICIOUS REGIONS DETECTED PER IMAGE BY THE PROPOSED METHOD, METHOD USED BY HU *et al.* [10], CAO *et al.* [17], AND THE GROUND TRUTH PROVIDED BY MIAS

Mammogram ID	Class of lesions	Proposed method	Hu *et al.*	Cao *et al.*	Ground Truth	Mammogram ID	Class of lesions	Proposed method	Hu *et al.*	Cao *et al.*	Ground Truth
mdb001	CIRC	1	1	1	1	mdb110	ASYM	2	1	3	1
mdb002	CIRC	2	1	1	1	mdb111	ASYM	1	1	2	1
mdb015	CIRC	1	4	8	1	mdb115	ARCH	2	1	1	1
mdb017	CIRC	2	5	3	1	mdb117	ARCH	1	1	3	1
mdb019	CIRC	2	2	7	1	mdb120	ARCH	1	2	2	1
mdb021	CIRC	1	1	7	1	mdb121	ARCH	1	1	2	1
mdb023	CIRC	2	4	4	1	mdb124	ARCH	1	1	2	1
mdb244	CIRC	2	1	4	1	mdb125	ARCH	2	2	4	1
mdb270	CIRC	4	2	9	1	mdb127	ARCH	2	3	4	1
mdb290	CIRC	2	3	1	1	mdb163	ARCH	1	1	2	1
mdb315	CIRC	1	1	1	1	mdb165	ARCH	1	1	1	1
mdb013	MISC	1	2	7	1	mdb170	ARCH	1	2	2	1
mdb030	MISC	3	6	10	1	mdb171	ARCH	3	3	1	1
mdb032	MISC	1	2	10	1	mdb145	SPIC	3	2	3	1
mdb058	MISC	1	2	4	1	mdb175	SPIC	2	3	1	1
mdb063	MISC	1	2	2	1	mdb178	SPIC	1	1	1	1
mdb264	MISC	1	1	1	1	mdb179	SPIC	1	1	1	1
mdb265	MISC	1	1	3	1	mdb181	SPIC	1	1	1	1
mdb072	ASYM	1	1	2	1	mdb186	SPIC	4	1	1	1
mdb081	ASYM	1	1	1	1	mdb188	SPIC	3	1	2	1
mdb083	ASYM	1	1	9	1	mdb190	SPIC	0	2	1	1
mdb090	ASYM	2	2	5	1	mdb191	SPIC	2	5	3	1
mdb099	ASYM	4	5	14	1	mdb193	SPIC	1	1	2	1
mdb102	ASYM	2	3	3	1	mdb198	SPIC	1	1	2	1
mdb104	ASYM	1	2	5	1	mdb199	SPIC	2	3	7	1
mdb105	ASYM	1	1	4	1	mdb202	SPIC	1	1	1	1
mdb107	ASYM	1	2	6	1	mdb207	SPIC	2	1	1	1

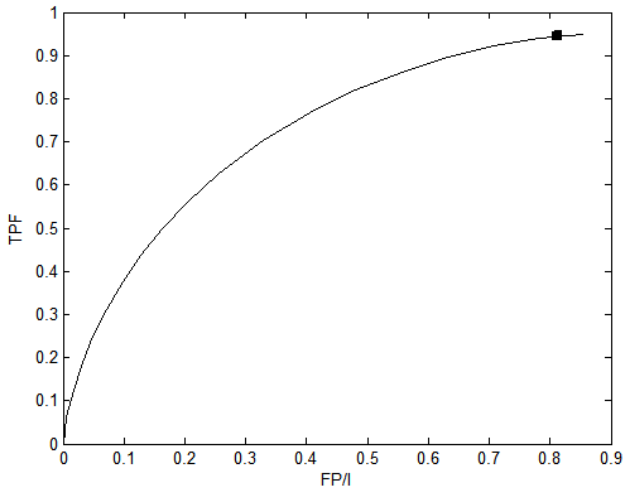

Fig. 4. FROC analysis

decreases the number of false detections which enhances the specificity of the proposed method. Following this the morphological filter performs a size and shape-dependent processing to enhance the regions with appearance similar to typical masses. This step is highly useful to target the candidate regions. However, since the morphological filter uses a circular structural element, it is more likely to enhance CIRC masses compared to SPIC masses and hence the algorithm has relatively lesser efficiency in the case of SPIC lesions. Finally, as masses have higher intensitiy values on a local scale, local thresholding proves to be pivotal for suspicious lesion segmentation in the proposed method. Fig. 5 shows the original mammograms and the corresponding final output images for four typical mammograms having lesions.

IV. CONCLUSION

This paper proposes an algorithm for the detection of space occupying lesions in digital mammograms using transition-invariant 2D wavelet transform . The proposed method involves adaptive thresholding on a global scale based on intensity level patterns of the image. The output is convolved with a morphologically enhanced output of the image reconstructed from 1^{st} level UWT coefficients. Thereafter, windows-based local thresholding is employed to segment the targets. The experimental results show that the proposed method is effective in detecting suspicious masses in mammograms at low false positive rates. The algorithm performs with a sensitivity of 94.56% at 0.81 false positives per image which is better compared to earlier reported method of Hu *et al.* [10]. The accuracy levels suggest that it can be used for the detection

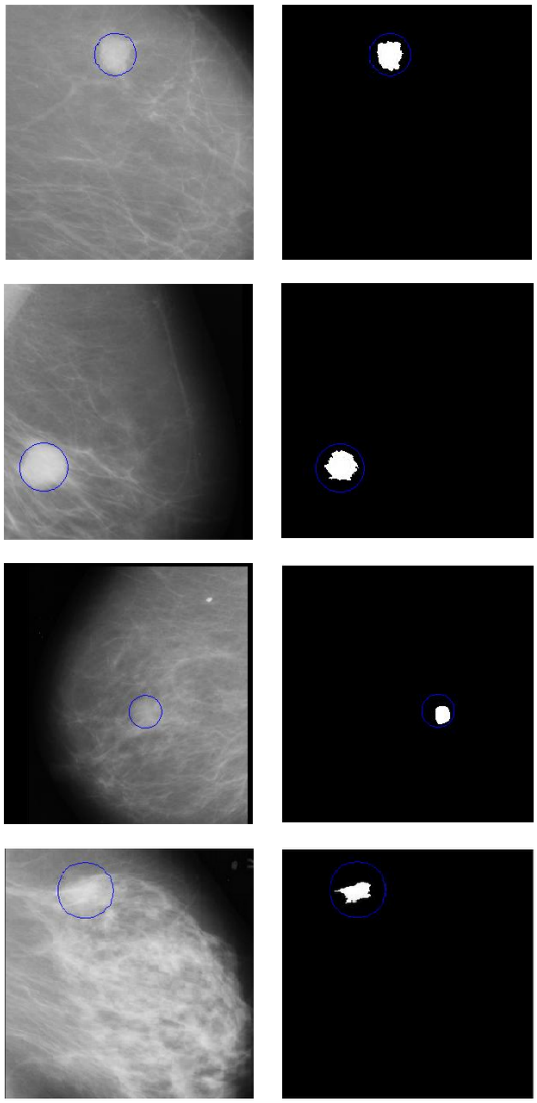

Fig. 5. From top to bottom–Detection results for mdb134, mdb028, mdb069 and mdb032. (a) Original mammogram (b) Final binary output after segmentation

of breast cancer in early stages. Also, in some cases where the masses do not fit in the regular criteria, some shape and texture-based features of masses can be further embedded in the algorithm to improve the efficiency.

REFERENCES

[1] World Cancer Report. Int. Agency for Research on Cancer. 2008. Retrieved 2011-02-26.

[2] Mette Kalager, "Effect of Screening Mammography on Breast-Cancer Mortality in Norway." New England Journal of Medicine. Sep. 2010.

[3] E.d. Pisano and F. Shtem, "Image processing and computer aided diagnosis in digital mammography: a clinical perspective," *Int. J. Pattern Recog. Artific. Intell.* vol. 7, no. 6, pp. 1493–1503, 1993.

[4] Li H., Wang Y., Liu K.J.R., Lo S.C., and Freedman M.T., "Computerized Radiographic Mass Detection – Part I: Lesion Site Selection by Morphological Enhancement and Contextual Segmentation," *IEEE Trans. Med. Imag.*, vol. 20, no. 4, pp. 289–301, Apr. 2001.

[5] M. Mohamed Fathima, D Manimegalai and S Thayalnayaki, "Automatic detection of tumor subtype in mammograms based On GLCM and DWT features using SVM," *International Conference on Information Communication and Embedded Systems (ICICES)*, pp. 809-813, Feb. 2013.

[6] Yong Zhang, Yihua Lan, Haozheng Ren, "Image Enhancement and Its Effects on Segmentation for Mammographic Masses," *Fifth International Symposium on Computaional Intelligence and Design (ISCID)*, vol. 1, pp. 423-426, Oct. 2012

[7] N. Karssemeijer and G. M. te Brake, "Detection of stellate distortions in mammogram," *IEEE Trans. Med. Imag.*, vol. 15, no. 1, pp. 611–619, Oct. 1996

[8] X. P. Zhang and M. D. Desai, "Segmentation of bright targets using wavelets and adaptive thresholding," *IEEE Trans. Image Process.*, vol. 10, no. 7, pp. 1020–1030, Jul. 2001.

[9] G. Kom, A. Tiedeu, and M. Kom, "Automated detection of masses in mammograms by local adaptive thresholding," *Comput. Biol. Med.*,vol. 37, no. 1, pp. 37–48, Jan. 2007.

[10] Kai Hu, X. Gao and Fei Li, "Detection of Suspicious Lesions by Adaptive Thresholding Based on Multiresolution Analysis in Mammograms," *IEEE Trans. Instrum. Meas.*, vol. 60, no. 2, pp. 462–472, Feb. 2011.

[11] A Mencattini, G Rabottino, M Salmeri, and R Lojacono, "Assessment of a Breast Mass Identification Procedure Using an Iris Detector," *IEEE Trans. Instrum. Meas.*, vol. 59, no. 10, pp. 2505-2512, Oct. 2010.

[12] Mencattini, M. Salmeri, R. Lojacono, M. Frigerio, and F. Caselli, "Mammographic images enhancement and denoising for breast cancer detection using dyadic wavelet processing," *IEEE Trans. Instrum. Meas.*, vol. 57, no. 7, pp. 1422–1430, Jul. 2008.

[13] J. L. Starck, J. Fadili, and F. Murtagh, "The Undecimated Wavelet Decomposition and its Reconstruction," *IEEE Transactions on Image Processing*, Vol. 16, no. 2, pp. 297-309, Feb. 2007.

[14] J. Nagi, S.A. Kareem, F. Nagi and S. K. Ahmed, "Automated Breast Profile Segmentation for ROI Detection Using Digital Mammograms," *IEEE EMBS Conference on Biomed. Engg & Sciences* , vol. 3, no. 11, pp. 87–92, Dec. 2010.

[15] F. Hess, M. Kraft, M. Rivhter, and H. Bockhorn, "Comparison and assessment of various wavelet and wavelet packet based denoising algorithms for noisy data," *Wavelet Dig.*, vol. 6, no. 2, http://www.rhrk.unikl.de/ mkraft/paper/ecmi96-paper252.ps, 1997.

[16] J. Suckling, S. Astley, D. Betal, N. Cerneaz, D. R. Dance,S.-L. Kok, J. Parker, I. Ricketts, J. Savage, E. Stamatakis, and P. Taylor, Mammographic Image Analysis Society MiniMammographic Database, 2005. [Online]. Available: http://peipa.essex.ac.uk/ipa/pix/mias/

[17] A. Z. Cao, Q. Song, and X. L. Yang, "Robust information clustering incorporating spatial information for breast mass detection in digitized mammograms," *Comput. Vis. Image Understand.*, vol. 109, no. 1, pp. 8696, Jan. 2008.

[18] Metz CE. Receiver operating characteristic (ROC) analysis: a tool for quantitative evaluation of observer performance and imaging systems. *JACR - Journal of the American College of Radiology* 3: 413–422, 2006